

# The X-Shooter Diaphragm Mode

Nov 29 - Dec 6, 2013

Jens-Kristian Krogager  
and  
Christophe Martayan



European Southern Observatory  
Santiago, Chile

## **Disclaimer**

All the observations were performed under technical time, usually under bad weather condition to test the limits and capabilities of the X-shooter diaphragm mode. It is not (yet) foreseen to offer this mode to the community but it opens some windows towards “well” known objects with properties or spectra not yet known in some wavelength range. The reduced data is offered without guarantee about its quality even if the intent was to provide the best possible spectra.

## **Introduction**

The X-shooter spectrograph at Paranal delivers medium resolution spectra covering wavelengths from U to K band simultaneously. X-shooter effectively works as three echelle spectrographs observing at the same time by the use of dichroic filters to split the light into the three separate arms: UVB covering 300 – 550 nm, VIS covering 550 – 1000 nm, and NIR covering 1000 – 2500 nm. Currently, the instrument is limited to targets fainter than roughly magnitude 3 in all bands.

The diaphragm mode for X-shooter is designed to allow observations of brighter targets than what is currently possible, thereby securing some of the first infrared spectra of nearby, bright stars. This is achieved by using a pinhole in the entry of the spectrograph to limit the amount of light reaching the detector. This pinhole mask is usually used for calibrations only, but when inserted during an exposure the pinhole works as a diaphragm to remove most of the flux and thus prevents the detectors from saturating.

In the following report, I will present the results of several tests carried out with the diaphragm mode of X-shooter. These tests were aimed at characterizing the performance, limitations and optimal observing strategy for this mode.

## The Data

Data for this project were collected in three runs: two in July and one in December. The various data are summarized below.

Target	Exposure time / sec			Slit width
	NIR	VIS	UVB	
<b>2013 Jul 23:</b>				
HD196171	0.665	0.50	0.50	Narrow
HD196171	2.000	6.00	5.00	Narrow
$\alpha$ Centauri	0.665	0.25	0.25	Narrow
$\alpha$ Centauri	0.665	5.00	4.00	Narrow
$\alpha$ Centauri	0.665	5.00	4.00	Narrow
$\alpha$ Centauri	0.665	5.00	4.00	Narrow
$\alpha$ Centauri	0.665	5.00	4.00	Narrow
Antares	0.665	0.25	0.25	Narrow
Antares	0.333	0.25	0.25	Narrow
Antares	0.333	0.25	0.25	Narrow
Antares	0.665	3.00	3.00	Narrow
$\epsilon$ Scorpii	0.665	0.20	0.20	1", 0.9", 0.9"
$\epsilon$ Scorpii	0.665	0.25	0.25	Narrow
$\epsilon$ Scorpii	1.300	3.00	3.00	Narrow
$\epsilon$ Scorpii	2.000	6.00	10.0	Narrow
$\epsilon$ Scorpii	0.665	6.00	10.0	Narrow
$\epsilon$ Scorpii	0.665	6.00	10.0	Narrow
$\epsilon$ Scorpii	0.665	6.00	10.0	Narrow
$\epsilon$ Scorpii	0.665	6.00	10.0	Narrow
$\eta$ Scorpii	0.665	0.20	0.20	1", 0.9", 0.9"
$\eta$ Scorpii	4.000	10.0	10.0	Narrow
<b>2013 Jul 18:</b>				
Achernar	0.665	0.25	0.25	Narrow
Achernar	1.300	0.50	0.10	Narrow
Achernar	0.665	0.20	0.10	Narrow
<b>2013 Dec 6:</b>				
Fomalhaut	0.665	0.20	0.20	Narrow
Fomalhaut_sky	0.665	0.20	0.20	Narrow
Fomalhaut	0.660	0.20	0.20	Narrow
Achernar	0.660	0.20	0.20	Narrow
Achernar_sky	0.660	0.20	0.20	Narrow
Achernar_sky	0.333	0.20	0.10	5", 5", 5"
Achernar	0.333	0.20	0.10	5", 5", 5"
HD196171	0.660	0.20	0.20	Narrow
HD196171	0.660	0.20	0.20	Narrow
HD196171	0.660	0.20	0.20	5", 5", 5"
HD196171	0.660	0.20	0.20	5", 5", 5"

All data were obtained in 1x1 binning with fast readout (400k) for UVB and VIS. Calibration files were obtained on the same day as the science exposures. The slit width “narrow” refers to the configuration with the smallest possible slit in each arm, i.e., 0.5", 0.4", 0.4" for UVB, VIS and NIR, respectively. For other configurations, the used slit width is given for each arm in the following order: UVB, VIS, NIR.

## Acquisition and observation restriction

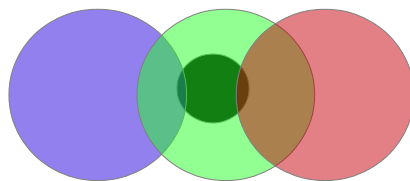
The instrument setup at the time of the acquisition is as follows:

- instrument shutter open
- calib side: telescope
- AG slide: pinhole instead of slot, it allows to diaphragm the light entrance of the spectrographs
- slits on spectrographs: 0.5" (UVB), 0.4" (VIS), 0.4" (NIR) or wider.

The AFC corrects the flexures. However during the observation, if set to AUTO then the tip-tilt mirrors will take into account the airmass to center the spectra. This will lead to a shift with respect to the position of the pinhole in the AG slide. In the normal slit observation, in the AG slide a slot is used therefore the shift is foreseen. Therefore the spectra will be slightly shifted. The other positions PARK or STAT should not be used.

The current centering algorithm will center the object taking into account the airmass to correct the atmospheric differential effect with respect to the reference centering positions. Those ones are based on the pinhole position in each filter. As such one has to manually fine-tune the centering of the object in the pinhole

Because of the use of the pinhole instead of the slot, some of the light is lost. It is even more the case in the wavelength different than the one of the acquisition filter as illustrated below.



In this example, the centering is performed in the green, some light is lost due to the size of the pinhole with respect to the PSF. The light coming from the blue and red wavelength is also strongly lost. However because the objects adapted of this mode are extremely bright this is not so an issue.

Actually in case of objects even too bright for the diaphragm mode, one can consider to use a specific filter for the centering to force some light to be lost. This would permit to do not saturate. For instance, if the object has a magnitude of -5 in U band even with the diaphragm mode it is still too bright for not saturating. As a consequence one can choose to use a red filter like the I band to center in this band and lose some light from the U band.

In the worse cases, if the object is extremely bright in all band one can consider to decenter the object in the direction perpendicular to the dispersion.

However this mode suffers from some restrictions:

- it is not possible to use the IFU because in the AG slide it is not possible to setup at the same time the pinhole and the IFU.
- The nodding mode is not really possible because it will center out the object.
- Therefore the possible observing mode are the stare, the GenericOffset and the fixedSkyOffset. However, the use of a sky position is not useful (see next sections) and the most suited template is the stare one.
- Due to the strong flux losses related to the pinhole and to the centring, no good flux calibration is possible (see next sections).

## Data Reduction

The data were reduced as regular slit exposures taken in “STARE” mode using the official esorex pipeline version 2.3.0. I started out by reducing one frame only to test a few options during the reduction. The first thing to test was the impact of reducing with sky subtraction (default) or without. I did these tests in the NIR arm, as the sky emission lines are most abundant here. There were no significant differences between the reductions with and without. The pipeline usually subtracts the sky from the region around the trace of the object; however, when using the pinhole all the sky background is blocked. The pipeline is therefore not able to model the sky spectrum and perform sky subtraction.

For the data taken December 6, we observed in so-called “offset” mode, in which an empty region of sky is observed after every science exposure. That way the observed sky spectrum can be subtracted during the reduction. However, the exposure times are so short that the skylines are not visible. It is therefore not possible, nor strictly necessary, to perform sky subtraction in these short exposure even when using the “offset” mode.

After establishing that sky-subtraction was not possible, all spectra were observed using the option `--sky-subtract=FALSE`. Some of the reduced 2D spectra showed strange artifacts along the edges of the trace resulting from the rectification process. These artifacts propagate into the extracted 1D spectra and leave small wiggles in the spectrum. By reducing the final pixel size in the spatial direction in the reduction (`--rectify-bin-slit`), the wiggles were reduced by a factor of two. I tested the reduction with various pixel sizes in the spatial dimension for the NIR arm: 0.21” (default), 0.25”, 0.10”, 0.05”, and 0.02”. The reductions with pixel sizes 0.10” and smaller all gave nearly the same output in terms of variance in the 1D spectrum, hence a smaller pixel size than 0.10” does not lead to any significant improvement. For VIS and UVB I used a final pixel size of 0.08” and 0.10”, respectively.

I also performed tests with varying spectral resampling and rectification kernels, however, none of these improved the final spectra. Figure 1 shows the artifacts from the rectification in the 2D spectra for each arm. It is not yet clear whether these effects are caused by observing through the pinhole or whether it is a consequence of observing such bright targets. This could be tested by reducing a target with similar count levels in the raw spectrum and see whether these effects are visible in the target observed with the regular slit observations. This was unfortunately not possible given the duration of this project.

All the reduced spectra will be available on the x-shooter webpage.

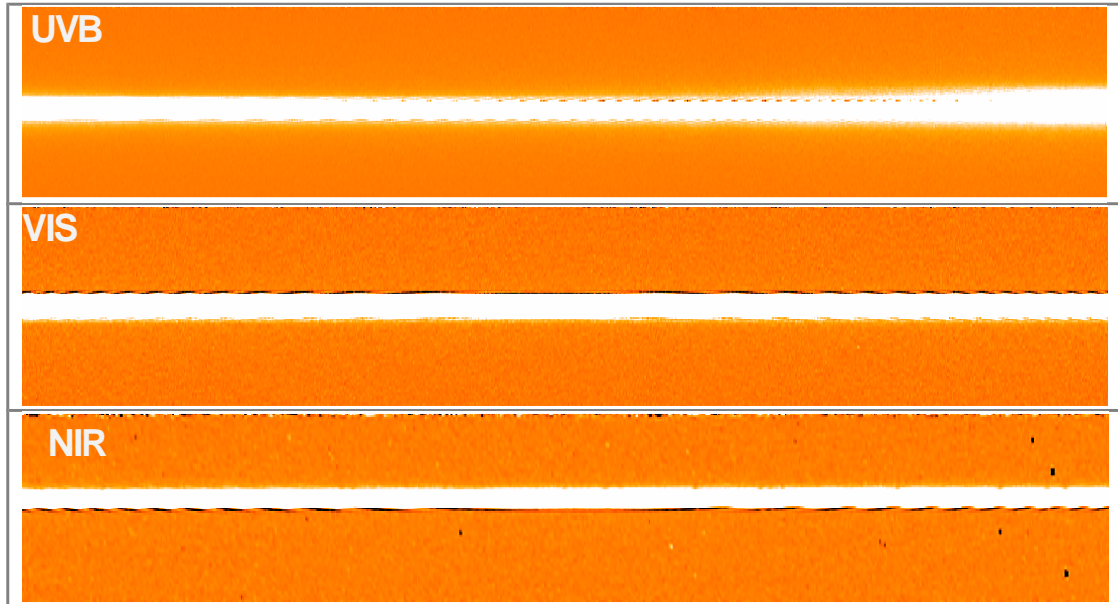


**Figure 1:** Cutouts of the final 2D spectrum for Achernar ( $V = 1.1$ ,  $K = -4.1$ ). The top panel shows the UVB arm from 435 – 450 nm, the middle panel shows the VIS arm from 770 – 785 nm, and the bottom panel shows the NIR arm from 1720 – 1755 nm. In the VIS and UVB arm, the wiggles are visible in the top edge of the trace. In the NIR arm, the wiggles are visible in the lower edge of the trace.

## Flux Calibration

Observing through the pinhole is designed to remove most of the light to allow observations of bright targets; however, this observation mode makes the flux calibration very difficult, as the exact amount of light passing through the pinhole is unknown. In order to test whether it was possible to flux calibrate the spectra, I used a response curve obtained from a previous reduction. This made it possible to make a quick estimate of the feasibility of the calibration. I tested the response curve on the target Antares, and was able to correct for the response of the instrument and detector.

Next step was to estimate the flux loss due to the pinhole mask. I did this by modeling the point-spread function (PSF) with a 2D Gaussian approximation and then comparing the total PSF flux to the amount of light passing through the pinhole opening (0.5"), which is located at fixed position on the CCD, depending on the filter of the AG camera. The PSF was determined from the acquisition image taken right before the science exposure. Since the PSF changes with wavelength, I had to take into account the wavelength dependence. The PSF wavelength-dependence can be broken down into two parts: (1) the FWHM scales as a power-law with wavelength:  $\text{FWHM} \propto \lambda^{-0.2}$ , and (2) the position of the PSF on the detector changes due to atmospheric dispersion. These effects are in theory straightforward to model, but the calculation relies on an accurate description of the PSF right before the science exposure. Given the lag between the acquisition image and the actual integration and the fact that the PSF changes very rapidly, the PSF measured in the acquisition image is not representative of the PSF during the short science exposure. Hence, flux calibration of targets in this mode is very challenging as the fraction of light lost due to the pinhole in each exposure is extremely hard to quantify. Observations with bad seeing conditions (seeing around 2"-3") should provide a PSF that makes

the loss calculation easier to perform, since the fraction of light passing through the pinhole will be more constant even though the extent of the PSF shifts due to time variations and atmospheric dispersion.

I tested this rough approximation with the reduction of Antares for which I also performed the response function test. The outline of the calculation is given below, and the result of this preliminary flux calibration is shown in Figure 2.

The PSF was fitted as a 2D Gaussian in the acquisition image taken immediately before the science exposure, using a PSF model of the following form:

$$\text{PSF} = A \exp \left[ -\frac{1}{2} \left( \frac{x-x_0}{\sigma_x} \right)^2 - \frac{1}{2} \left( \frac{y-y_0}{\sigma_y} \right)^2 \right],$$

where  $A$ ,  $x_0$ ,  $y_0$ ,  $\sigma_x$ , and  $\sigma_y$  in the general case are functions of wavelength. However, in this case the seeing was so bad that the central part of the PSF is approximately flat at the position of the pinhole (which is well known:  $x_p, y_p$ ) even though the target's position shifts over the CCD due to atmospheric dispersion.

This simplifies the calculation, as I don't have to take into account the shift of the PSF centroid. I can therefore calculate the pinhole loss since only the normalization of the PSF is wavelength dependent:

$$\int \int \text{PSF} \, dx dy = 2\pi A \sigma_x \sigma_y$$

The correction factor due to the pinhole loss is then simply given as the ratio:

$$r(\lambda) = \frac{F_{\text{pin}}}{\int \int \text{PSF} \, dx dy} = \frac{(D_{\text{pin}})^2}{8\sigma_x \sigma_y} \exp \left[ -\frac{1}{2} \left( \frac{x_p - x_0}{\sigma_x} \right)^2 - \frac{1}{2} \left( \frac{y_p - y_0}{\sigma_y} \right)^2 \right]$$

where  $\sigma_x$  and  $\sigma_y$  depend on wavelength given the power-law expressed above.

Using this correction factor as a function of wavelength, I corrected the fluxes from the flux-calibrated spectra from the pipeline. In Figure 2, I show the result of this correction compared to the broadband fluxes in B and V band from SIMBAD. The discrepancy between the V-band and the corrected spectrum is only a few percent (2%), though a bit larger in the B-band (~7%).

Although this correction worked out surprisingly well in this case, the NIR arm could not be calibrated because the NIR spectrum was completely saturated in this exposure. In the subsequent exposure, the pinhole was moved off center in order not to saturate the NIR detector. This worked as expected, but the shift of the pinhole with respect to the PSF centroid meant that the simple approximation explained above does not apply, since the outer regions of the PSF are more sensitive to the fast time variations and to the atmospheric dispersion. A test with a decentered exposure of Antares showed that this calculation indeed does not recover the flux very well; this is shown in Figure 3. In the overlap region between the NIR and VIS spectra, the flux in the NIR spectrum is a factor of four lower than the flux in the VIS spectrum.

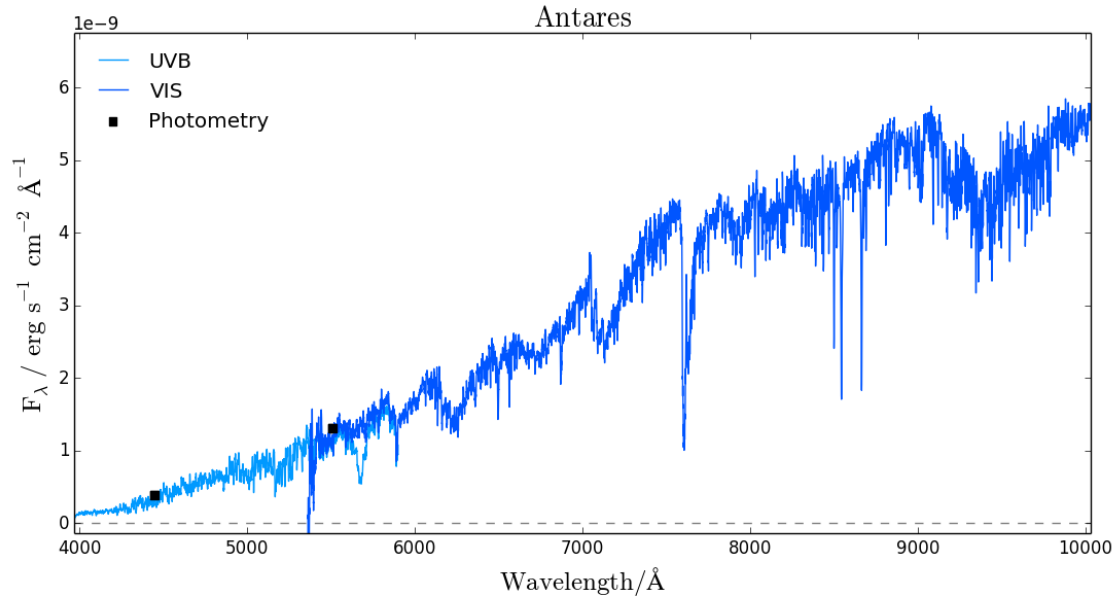


**Figure 2:** Preliminary results from flux calibration of Antares. UVB (light blue) and VIS (dark blue) spectra were only scaled by the flux-loss calculated from the PSF model. Photometry in B and V bands are shown as black squares. The spectrum has been smoothed for visual purposes.

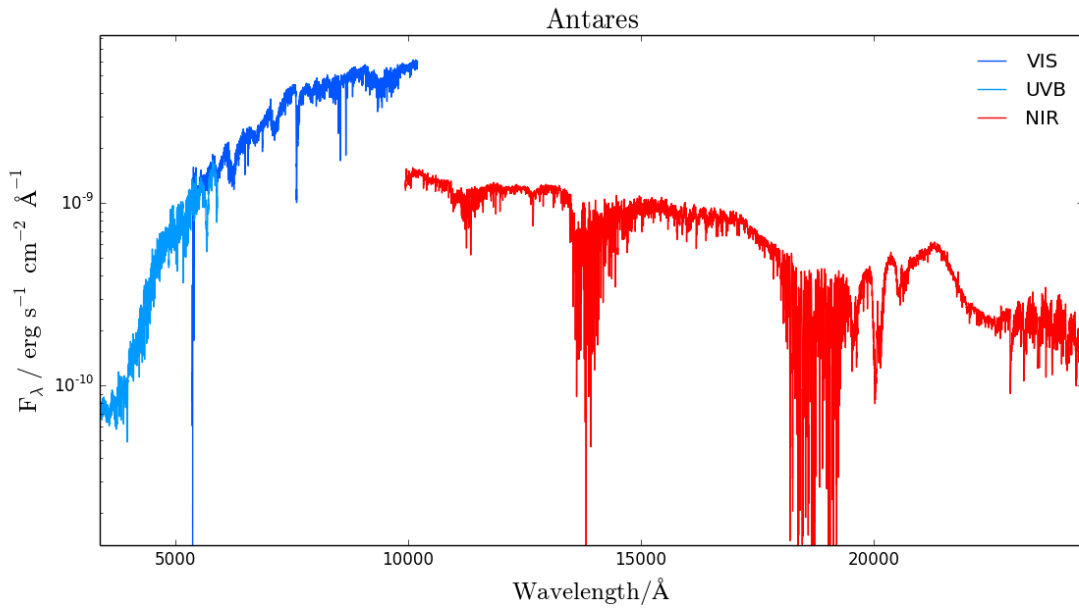


**Figure 3:** Comparison of the three spectra for Antares. The UVB and VIS spectra are the same as in Figure 2; however, the NIR arm is taken from a different exposure where the pinhole was moved away from the center of the target. The spectrum has been smoothed for visual purposes.

## PinholeAlignment

As mentioned above, the atmospheric dispersion affects the position of the PSF relative to the pinhole and hence introduces significant losses, depending on which wavelength is used for centering the pinhole on the object. This is illustrated in Figure 4, where the same object was observed twice: first time while centering in the  $U$ -band and second time while centering in  $g'$ . In the UVB spectra, the recovered flux differs significantly between the two exposures, but the differences in the VIS spectra are negligible. This excellent agreement between the two VIS spectra is very remarkable, since the two exposures were taken 6 minutes apart and with centering in two different bands. The spectra differ by only 2 – 5% over the entire VIS range. This must be caused by the observing conditions in the two exposure randomly being very similar.

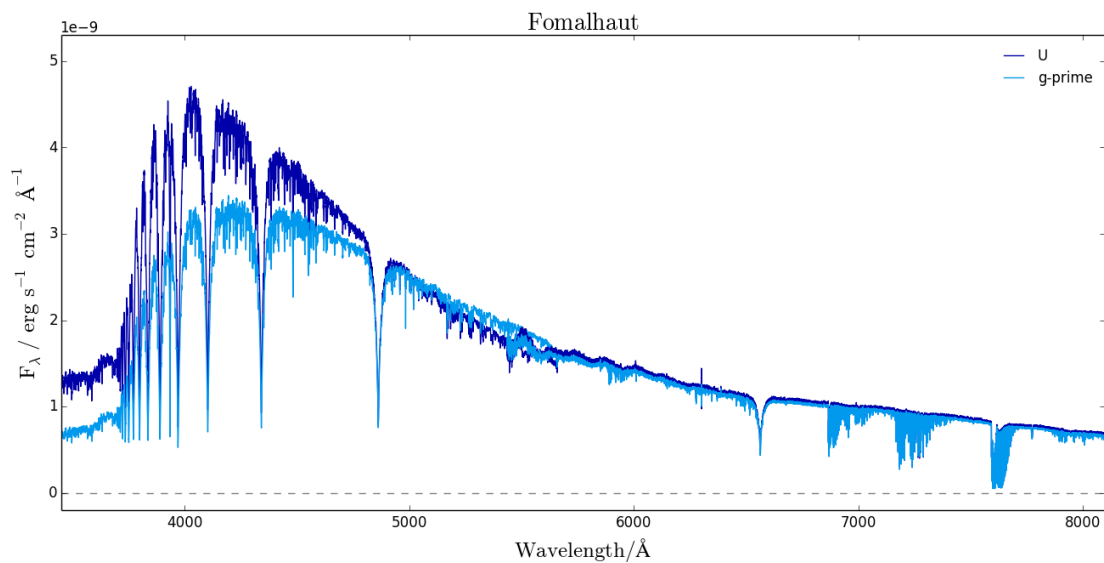


**Figure 4:** comparison of spectra with centering of the object performed in different bands. The dark and light blue lines show the flux-calibrated spectra where centering was done in  $U$  and  $g'$  bands, respectively.

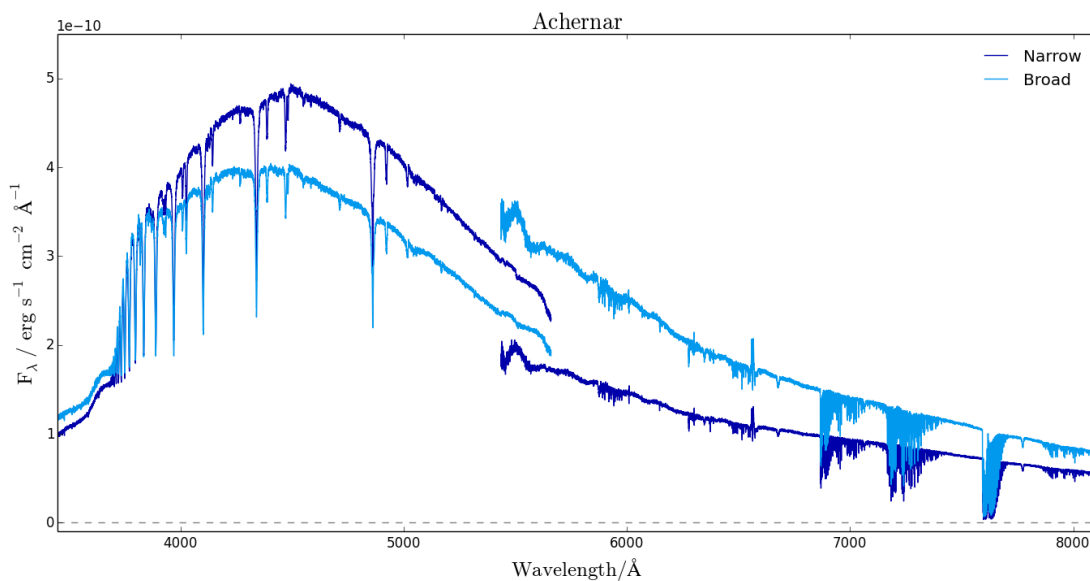


**Figure 5:** comparison of spectra with narrow and wide slit for Achernar obtained Dec 6, 2013, see table of data on first page. The light and dark blue lines show the spectra for wide and narrow slits, respectively.

The slit in each spectrograph introduces additional losses especially when using the narrow slits, since the pinhole may not be perfectly centered on the slit and for VIS and NIR the slit is narrower than the pinhole diameter, hence blocking even more light. In order to test the effect of the slit width on the recovered flux, we observed a star with two slit configurations: the first exposure was performed with the narrowest slits in each arm, the second was carried out with the widest (5'') slits in all arm. The flux-calibrated spectra are shown in Figure 5. The VIS spectra show, as expected more flux in the exposure with the widest slit, since less light is dispersed outside the slit. However, the UVB spectra show the opposite trend, i.e., the spectrum taken with the narrow slit configuration has *higher* flux. The centering was performed in *U*-band for the first exposure, but two sky frames were taken in between the science exposures and it is therefore very possible that the centering was not exactly the same in the second exposure. Moreover, the atmospheric conditions vary quickly and have a large impact on such short exposures. Hence, a direct quantitative analysis of these exposures is not meaningful. Nevertheless, the test does show that a wider slit recovers more flux as expected. This means that observing with the wide slit will reduce the impact of differential slit-loss without a loss in spectral resolution, as the resolution will be determined by the diameter of the pinhole.

## Conclusions

In this report, I have presented the preliminary tests and data for the X-shooter diaphragm mode. Below I will summarize and conclude on each individual section.

### Observational Strategy

In order to get the best possible understanding of each scientific exposure with this mode, it is important to have an acquisition image taken as close in time to the science exposure as possible. That way the pinhole loss and seeing can be estimated. Though this depends much on the specific conditions at the time of integration, as the short exposures are very sensitive to the time variations of the PSF, the acquisition image can - at least in some cases - help to characterize the observations. Moreover, the images provide information about what filter was used to center the image, which is crucial to the understanding of differential losses over the full spectral range.

### Reduction

The best reduction was obtained by turning off sky-subtraction (to gain a little speed) and by rectifying the spectra on to a finer grid than the default. However, the spectra still show artifacts in both the 1D and 2D spectra.

Sky subtraction is not possible, nor needed, since the exposure times are kept very short to keep the detectors from saturating.

### Flux Calibration

In general, it is not possible to obtain a good flux calibration due to the many unknown variables contributing to each exposure, e.g., time variations of the PSF, atmospheric dispersion, and slit-loss. It should therefore be noted that observing with the diaphragm mode should *not* be used in science cases that rely on a very accurate flux calibrations.

### Limiting Magnitudes

The normal limit for X-shooter is around magnitude +3 in all bands. With the diaphragm mode, we have been able to observe targets ranging from magnitudes 2.26 to -4.10 in *K*-band. In order to observe targets at the extremely bright end we observed during very bad seeing (FWHM  $\approx 3-4''$ ) and with the pinhole moved off the center of the target to limit the flux entering the instrument. The trade-off by observing such bright targets is that the absolute flux-calibration is very uncertain. The exact limit is very hard to quantify since it depends strongly on the pinhole position relative to the PSF during the exposure. With regular seeing of FWHM  $\sim 1''$ , a conservative limiting magnitude would be around 1 mag.

Nevertheless, the diaphragm mode makes it possible to observe thousands of stars with magnitudes brighter than the limit for regular spectroscopy with X-shooter, thereby securing some of the first infrared spectra for many of these stars with high quality for studying absorption lines and atmospheric phenomena in these stars.